Supporting Information for

Impact of a poly(ethylene glycol) corona block on drug encapsulation during polymerization induced self-assembly

Guanrui Li, Cassie Duclos, and Ralm G. Ricarte

Department of Chemical and Biomedical Engineering, FAMU-FSU College of Engineering, Tallahassee, FL 32310

Email: rricarte@eng.famu.fsu.edu

Table of Contents

S1. Dynamic light scattering (DLS) plots

Figures S1 and S2 detail the DLS g_2 autocorrelation functions and Γ vs. q^2 plots, respectively, for PEG solutions.

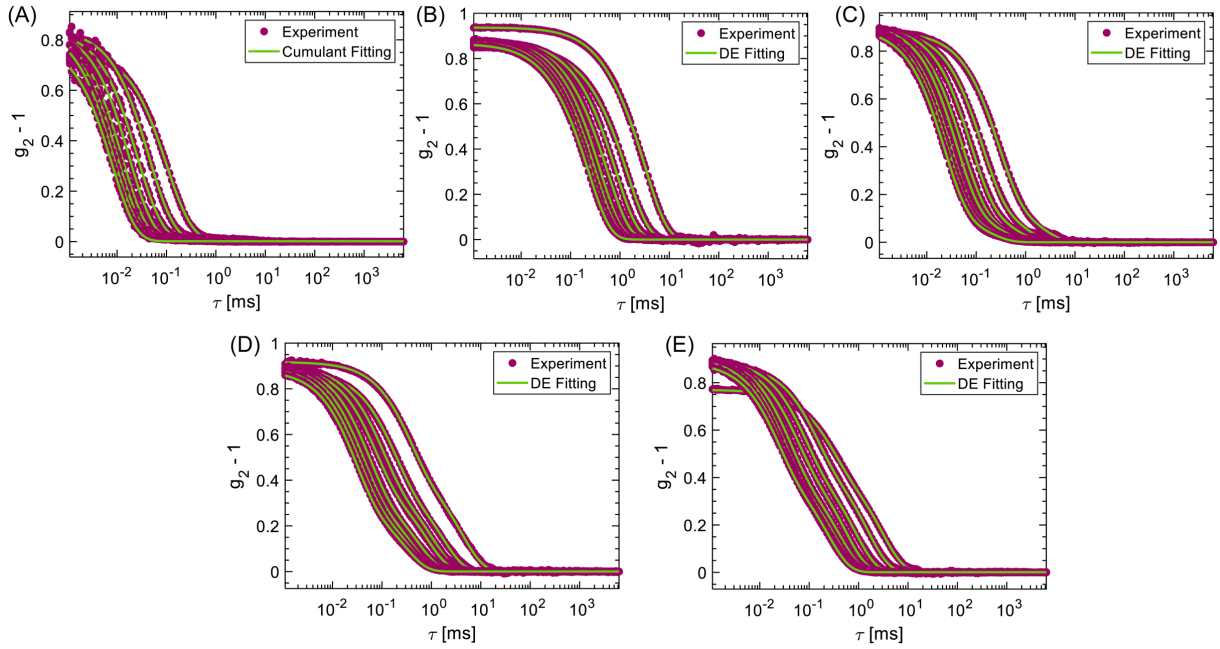

Figure S1. DLS g_2 autocorrelation functions for (A) PEG-OH, (B) PEG 0, (C) PEG 10, (D), PEG 16, and (E) PEG 20. Eqn. 2 is fit to (A) data, and Eqn. 3 is fit to (B) to (E) data

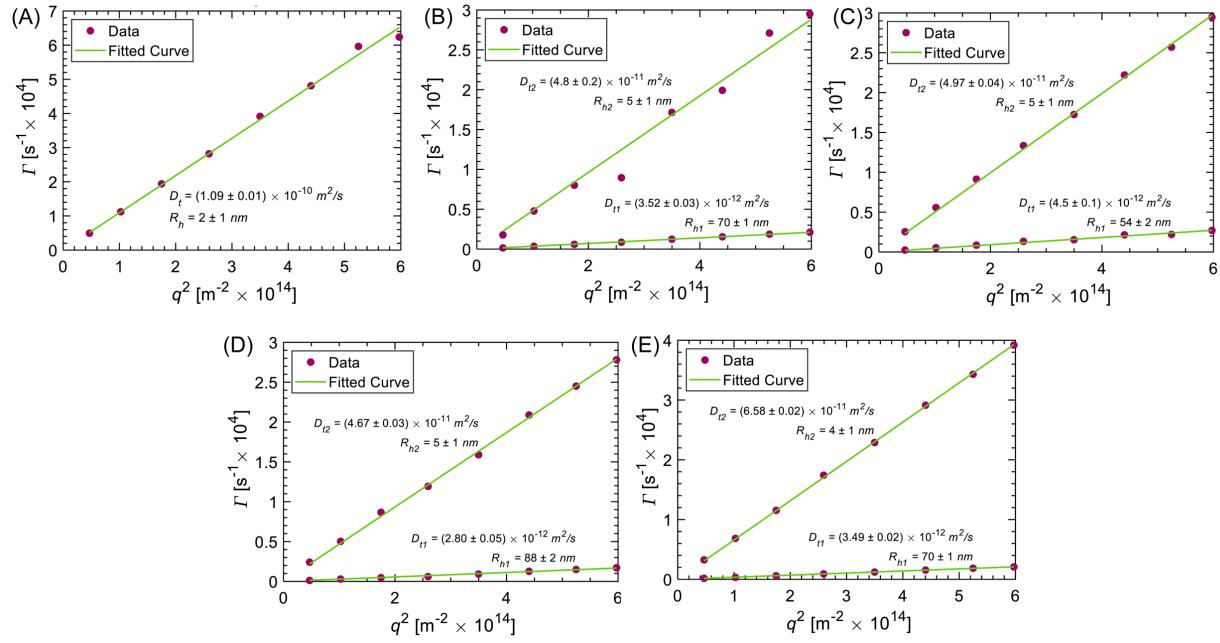

Figure S2. DLS Γ vs. q^2 for (A) PEG-OH, (B) PEG 0, (C) PEG 10, (D), PEG 16, and (E) PEG 20. Eqn. 2 is fit to (A) data, and Eqn. 3 is fit to (B) to (E) data.

Figures S3 and S4 detail the DLS g_2 autocorrelation functions and Γ vs. q^2 plots, respectively, for the diluted PEG-PHPMA PISA solutions.

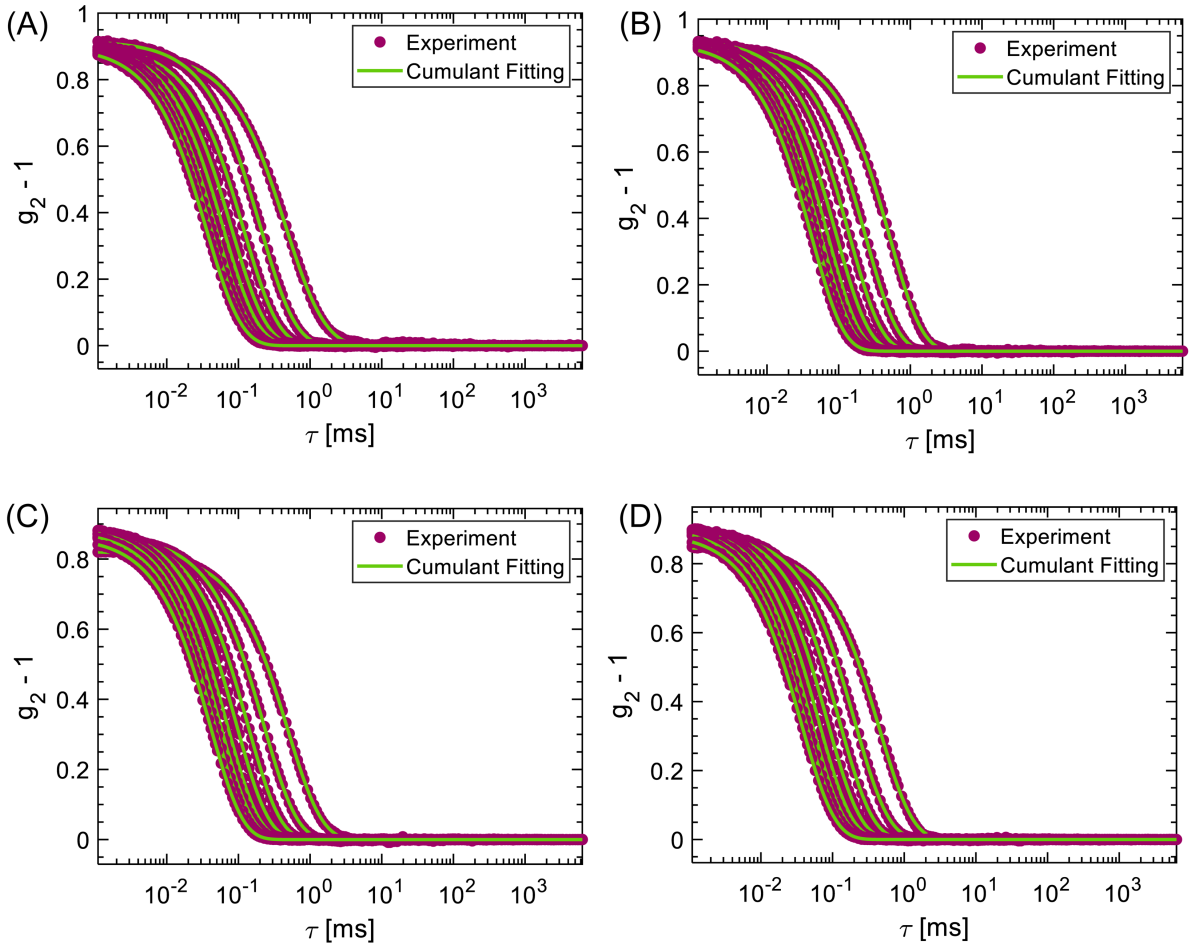

Figure S3. DLS g_2 autocorrelation functions for (A) PEG-PHPMA, (B) PEG-PHPMA 10, (C), PEG-PHPMA 16, and (D) PEG-PHPMA 20. Eqn. 2 is fit to data

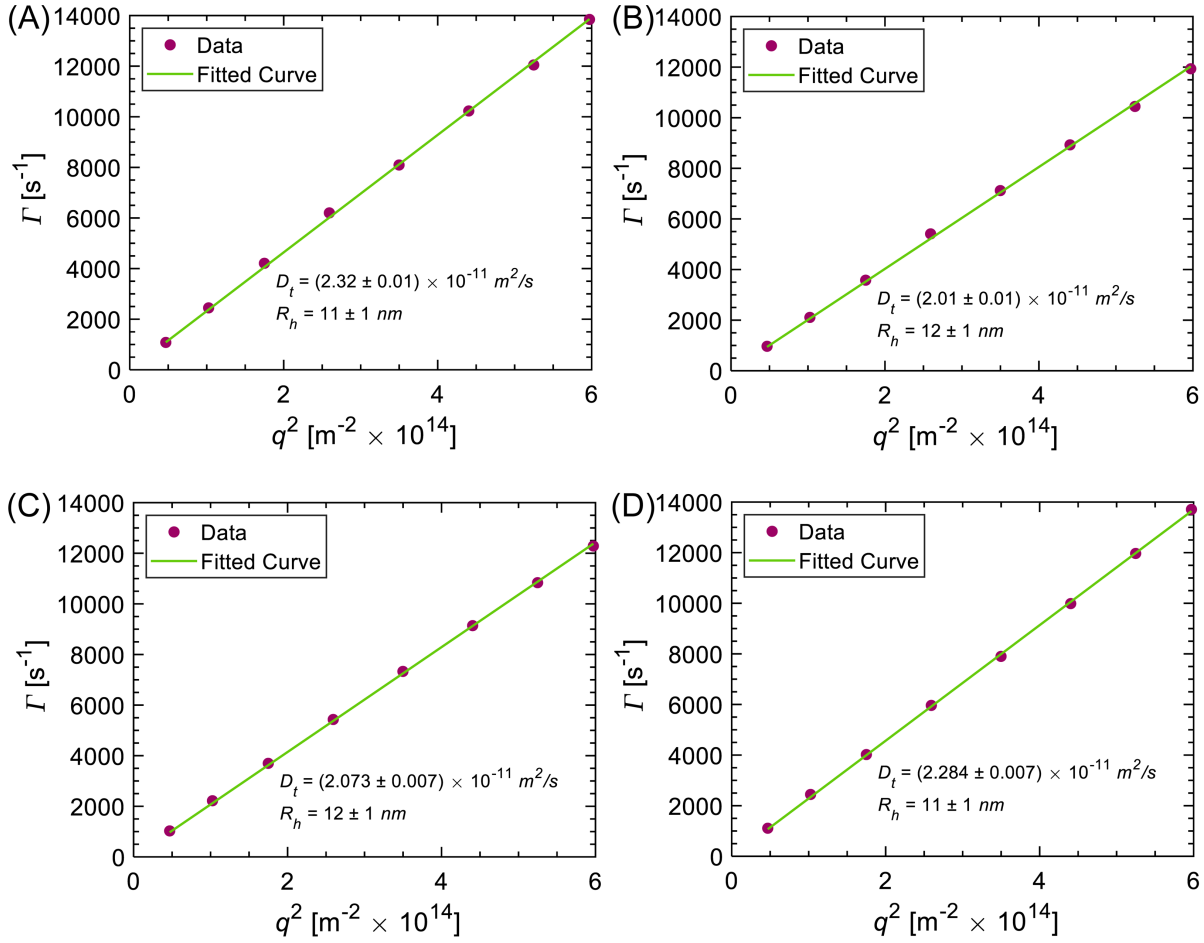

Figure S4. DLS Γ vs. q^2 for (A) PEG-PHPMA, (B) PEG-PHPMA 10, (C), PEG-PHPMA 16, and (D) PEG-PHPMA 20. Eqn. 2 is fit to data

S2. ^{1}H nuclear magnetic resonance (NMR) spectra

Figures S5 to S13 are the ^{1}H NMR spectra for PA, PEG, and PEG-PHPMA PISA solutions.

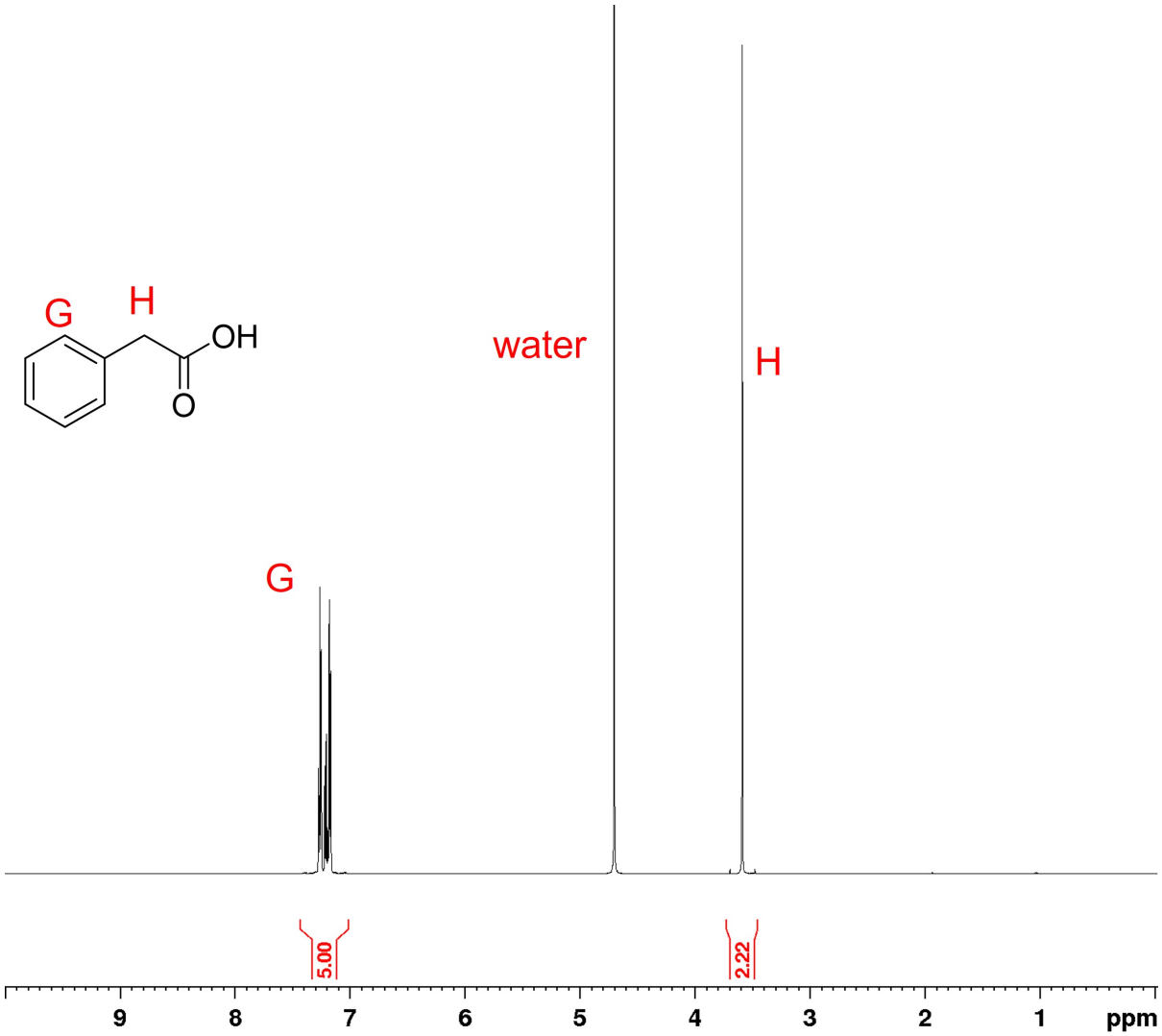

Figure S5. ^{1}H NMR spectrum of 16 mg/mL of phenylacetic acid in D_2O

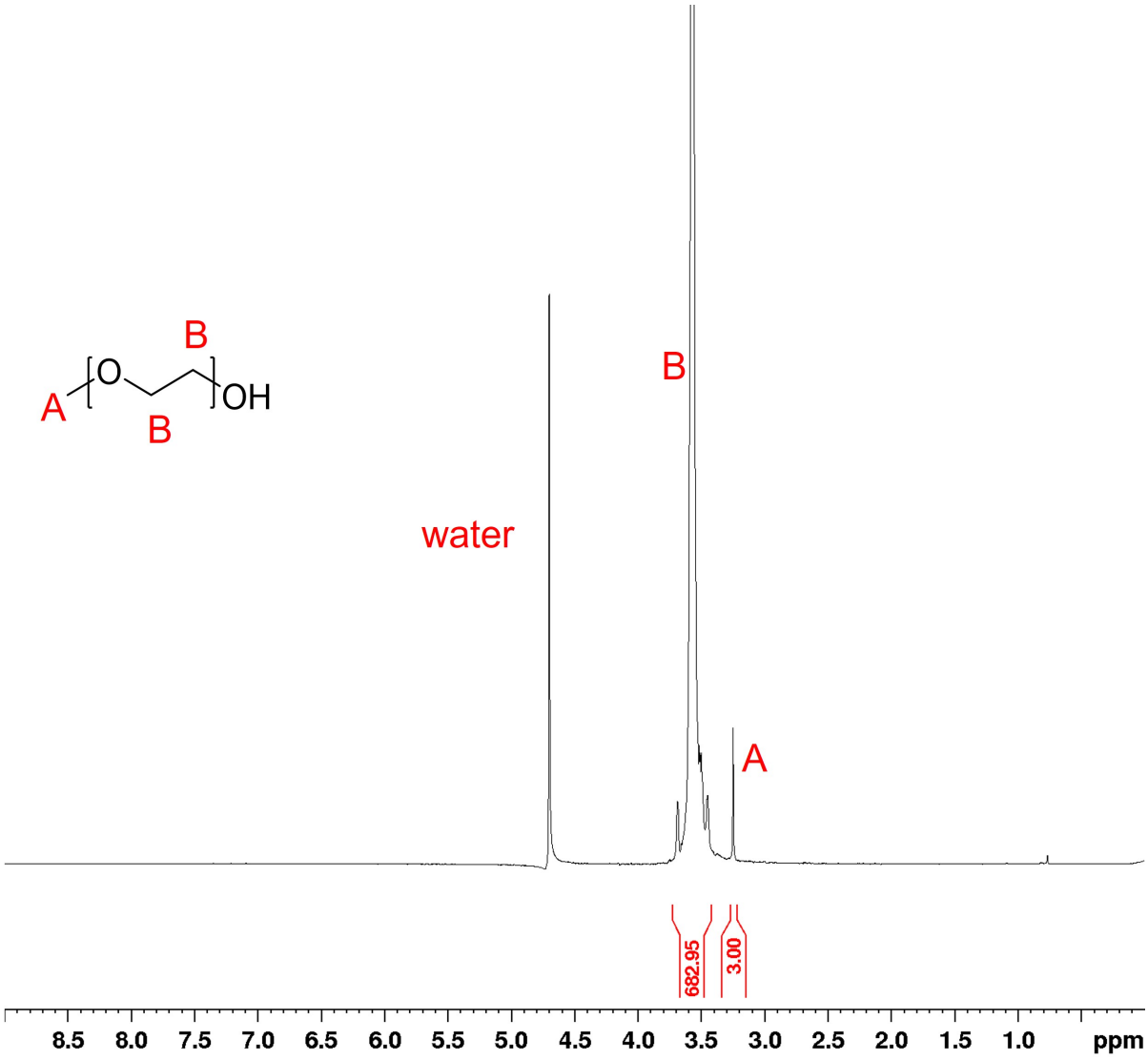

Figure S6. ^{1}H NMR spectrum of PEG-OH in D_2O

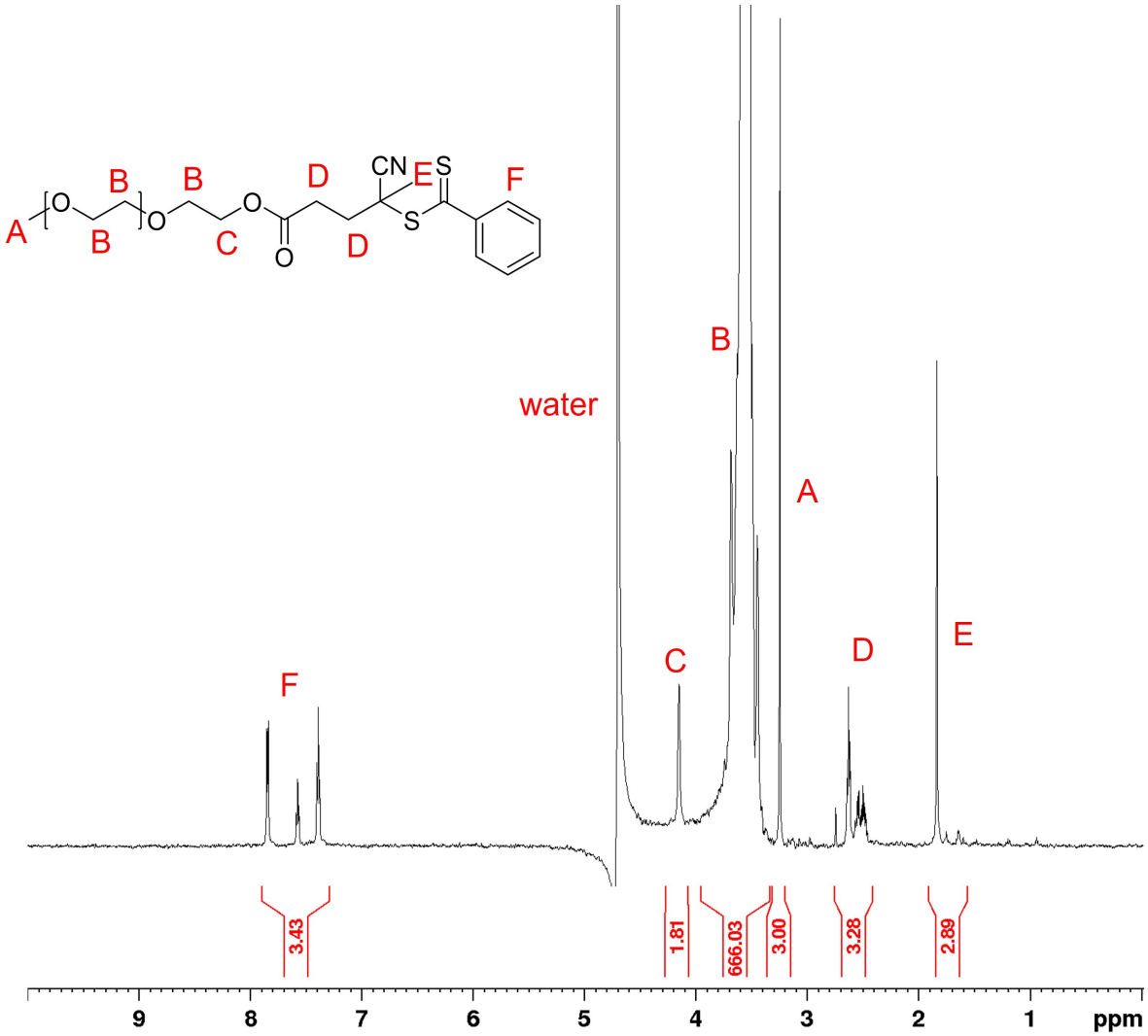

Figure S7. ^{1}H NMR spectrum of PEG 0 in D_2O

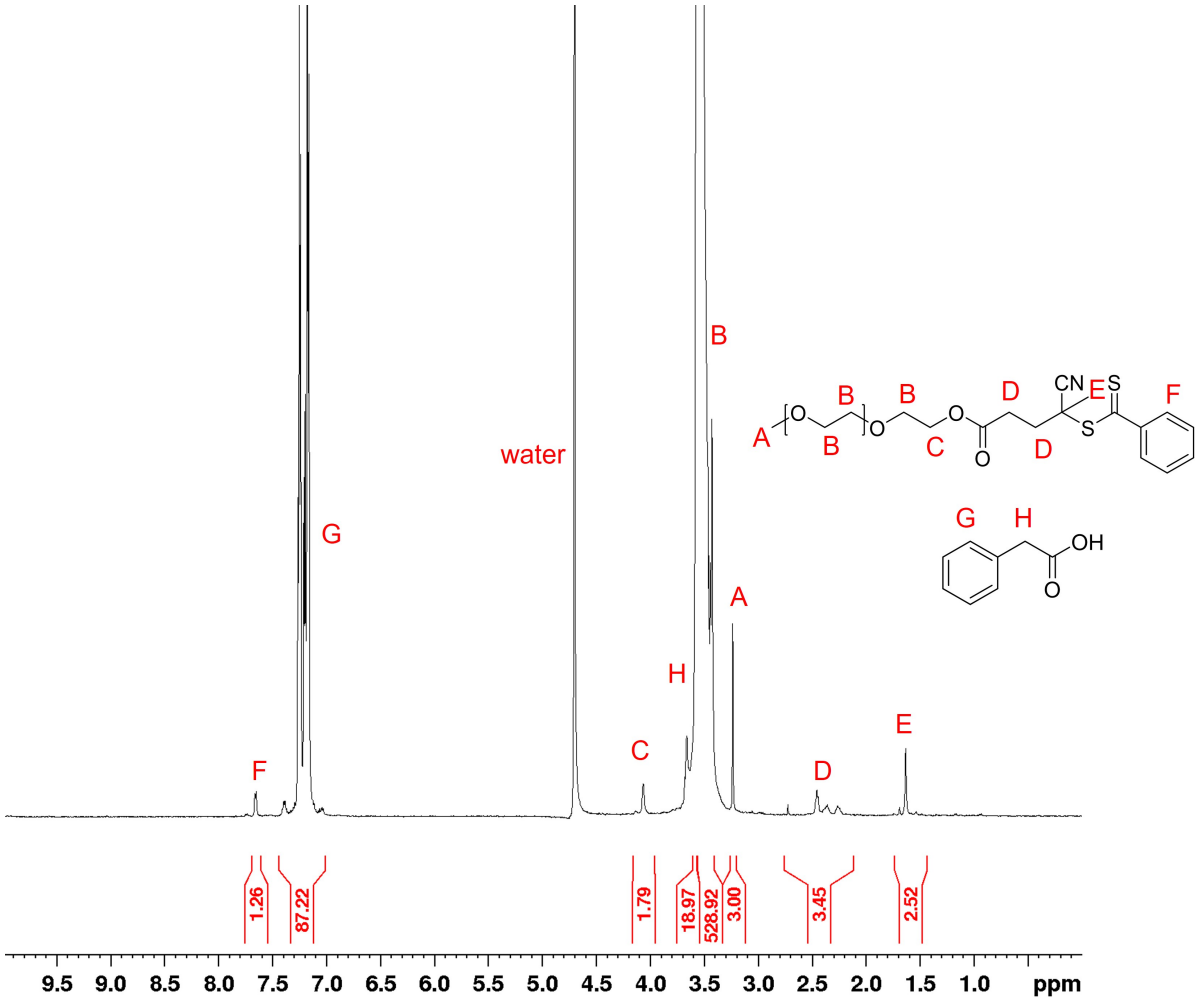

Figure S8. ^{1}H NMR spectrum of PEG 10 in D_2O

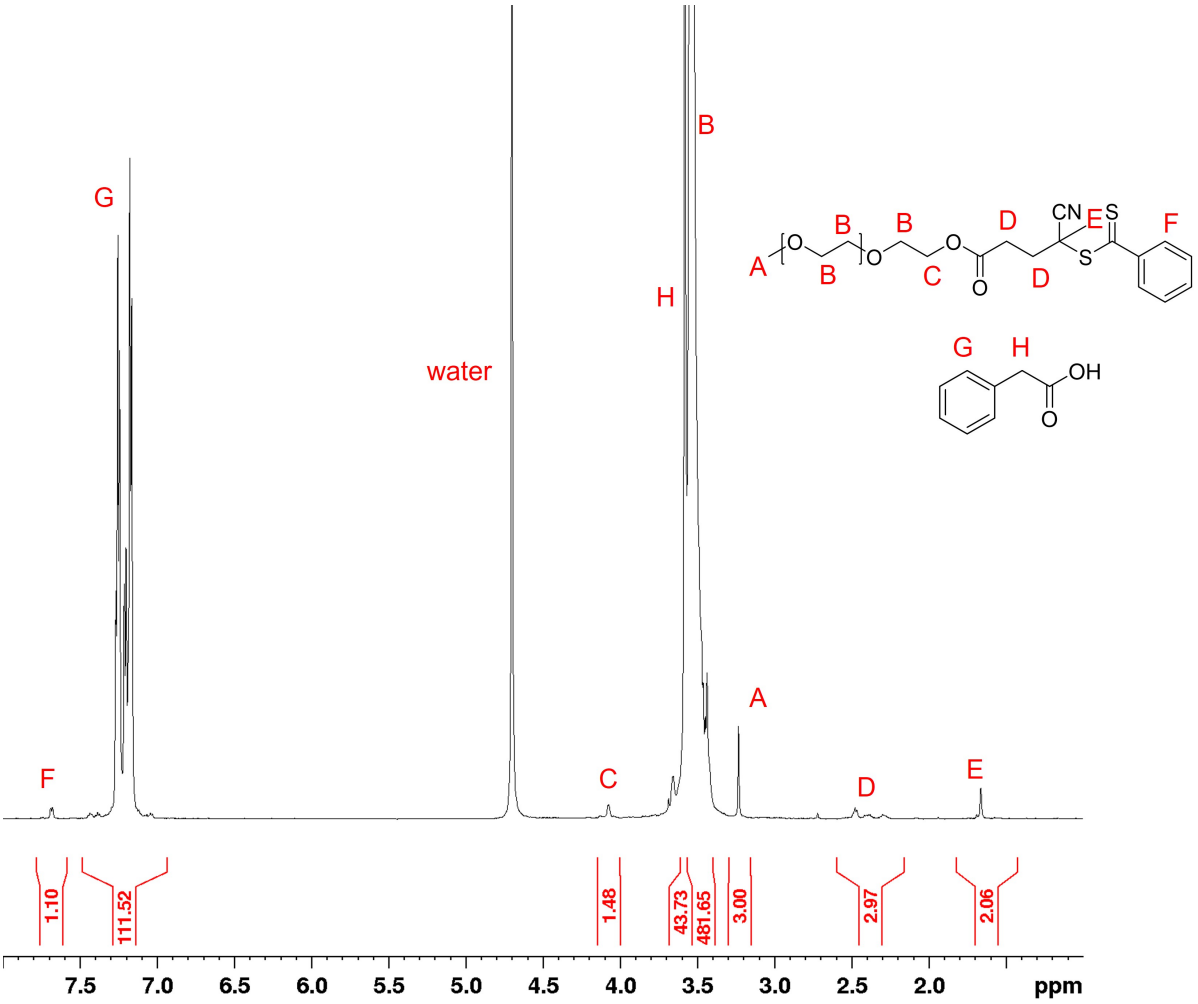

Figure S9. ^{1}H NMR spectrum of filtered PEG 16 in D_2O

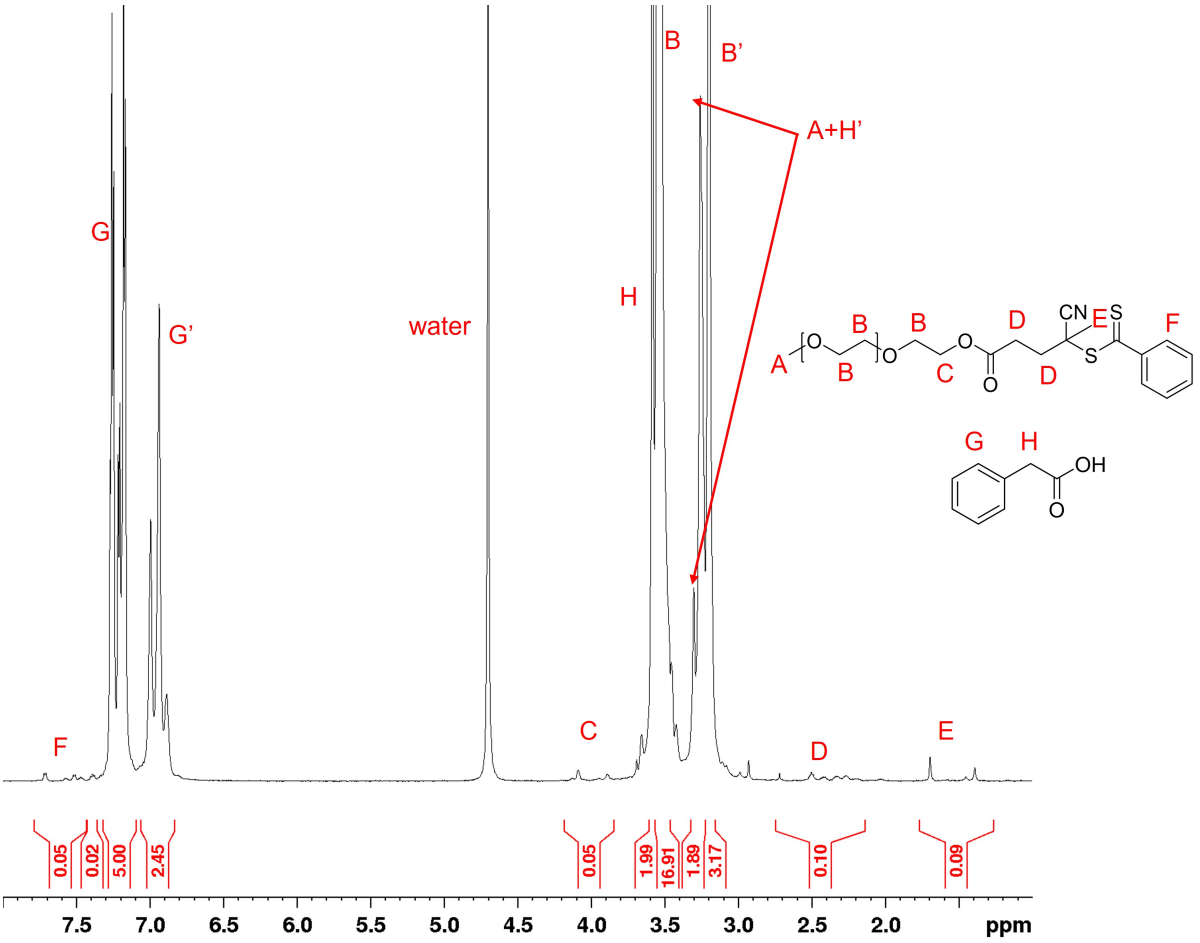

Figure S10. ^{1}H NMR spectrum of PEG 20 in D_2O

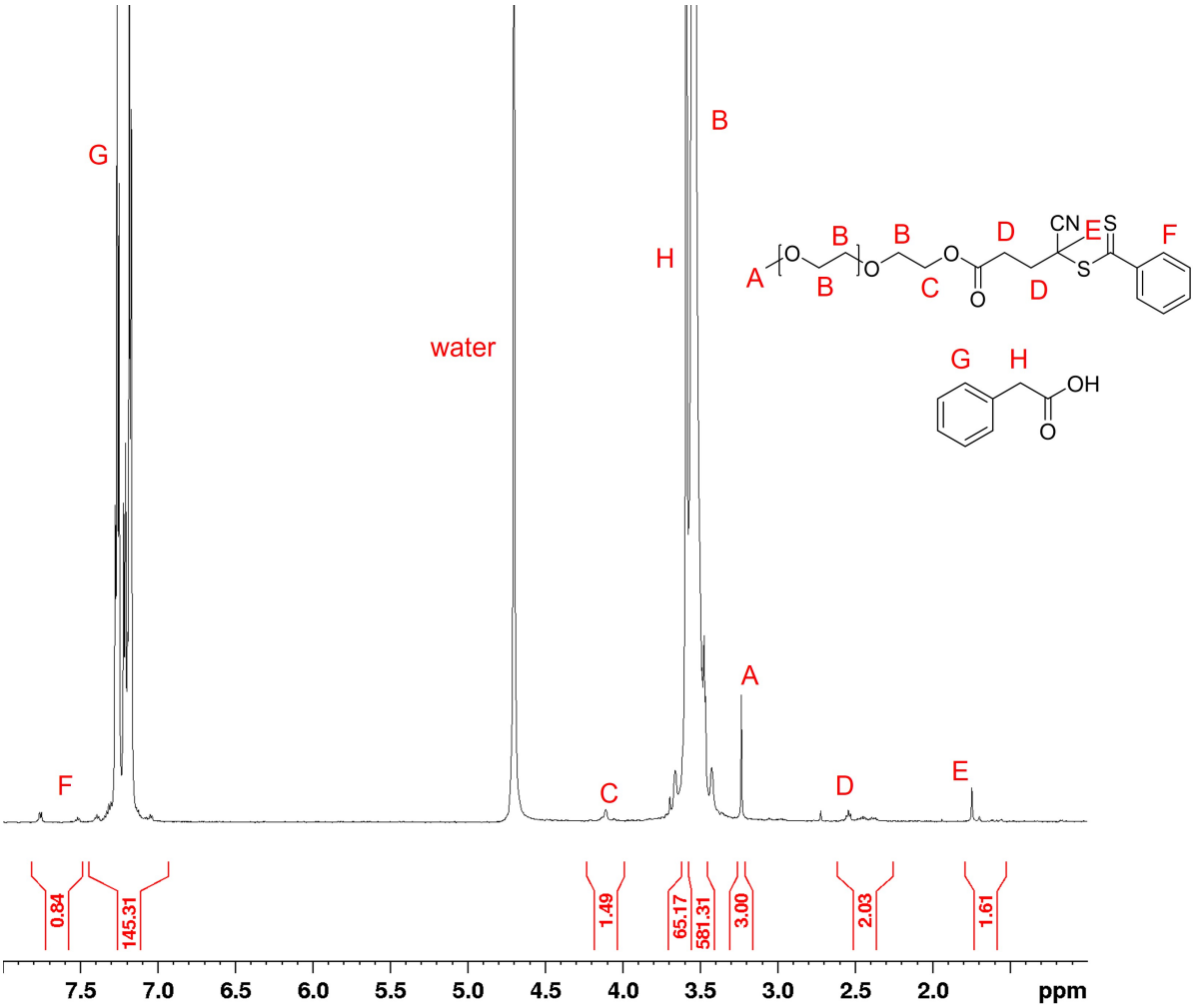

Figure S11. ^{1}H NMR spectrum of filtered PEG 20 in D_2O

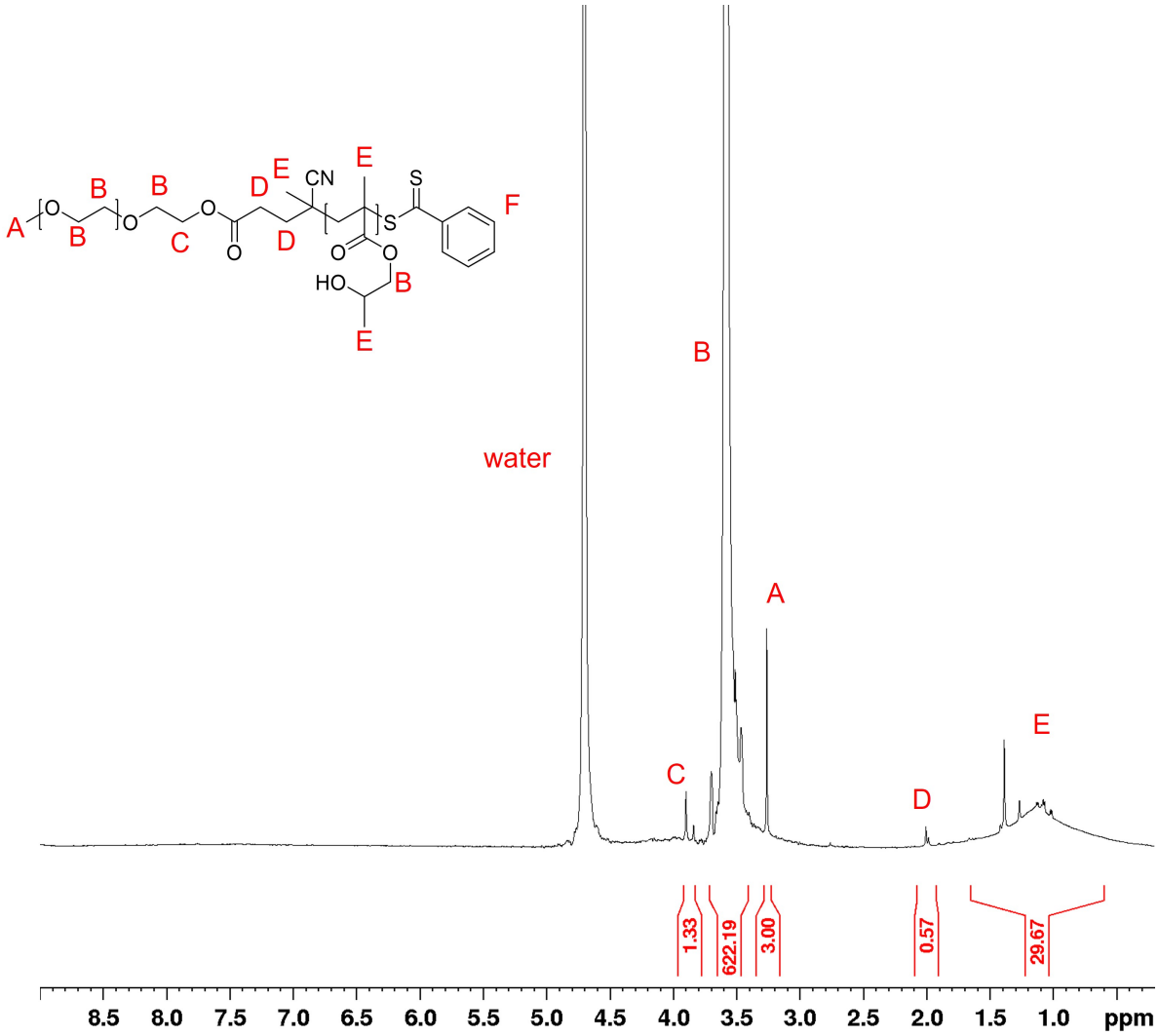

Figure S12. ^{1}H NMR spectrum of PEG-PHPMA 0 in D_2O

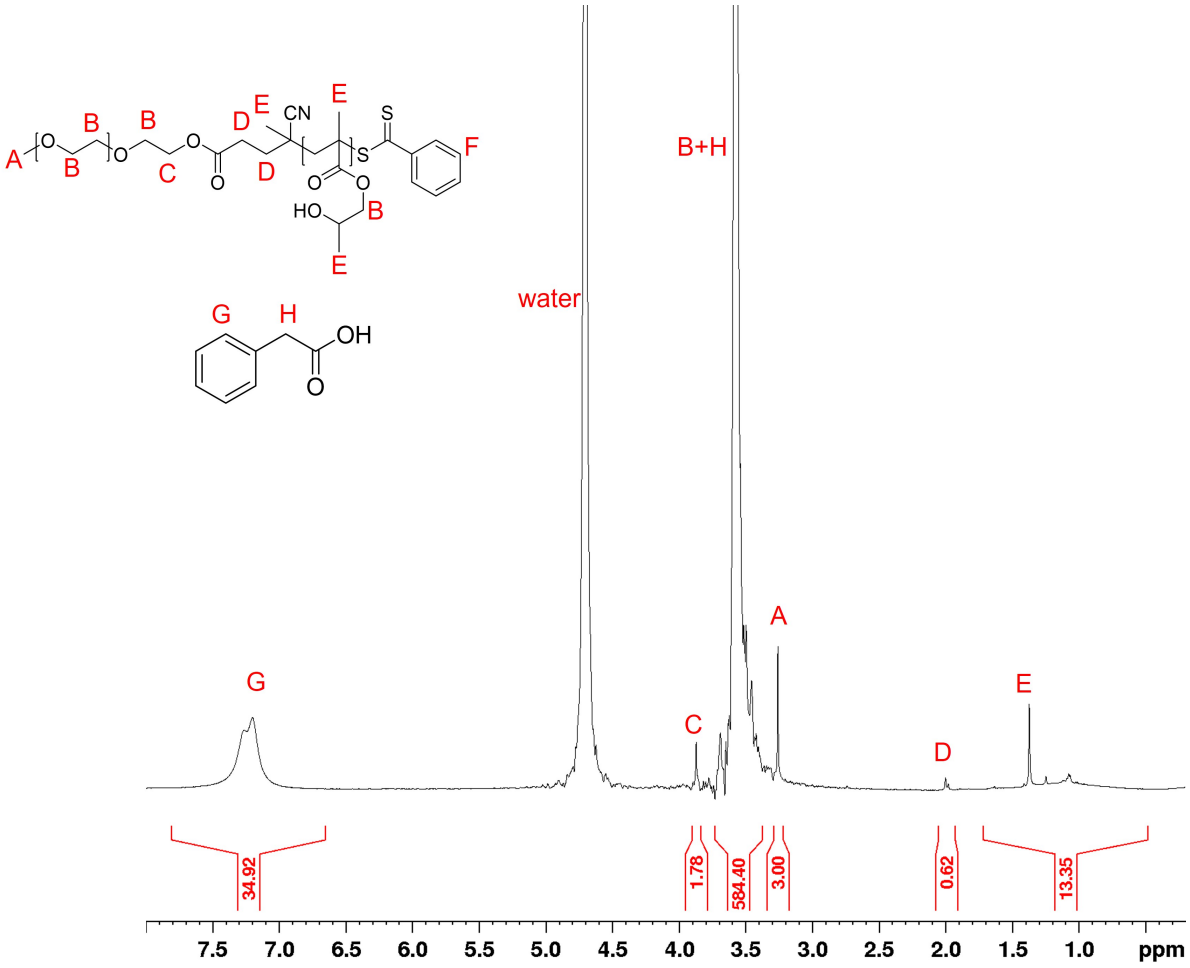

Figure S13. ^{1}H NMR spectrum of PEG-PHPMA 10 in D_2O

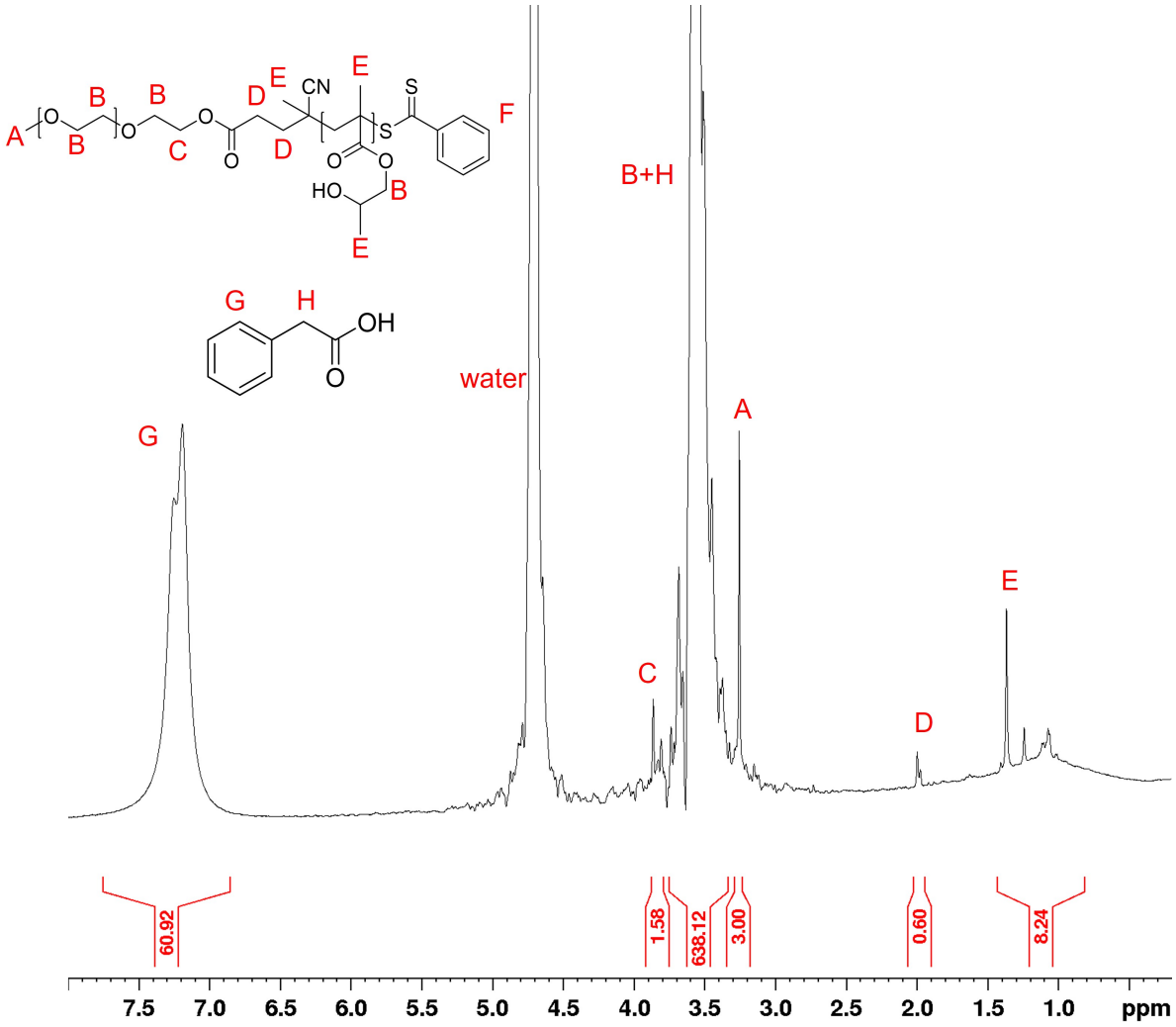

Figure S14. ^{1}H NMR spectrum of PEG-PHPMA 16 in D_2O

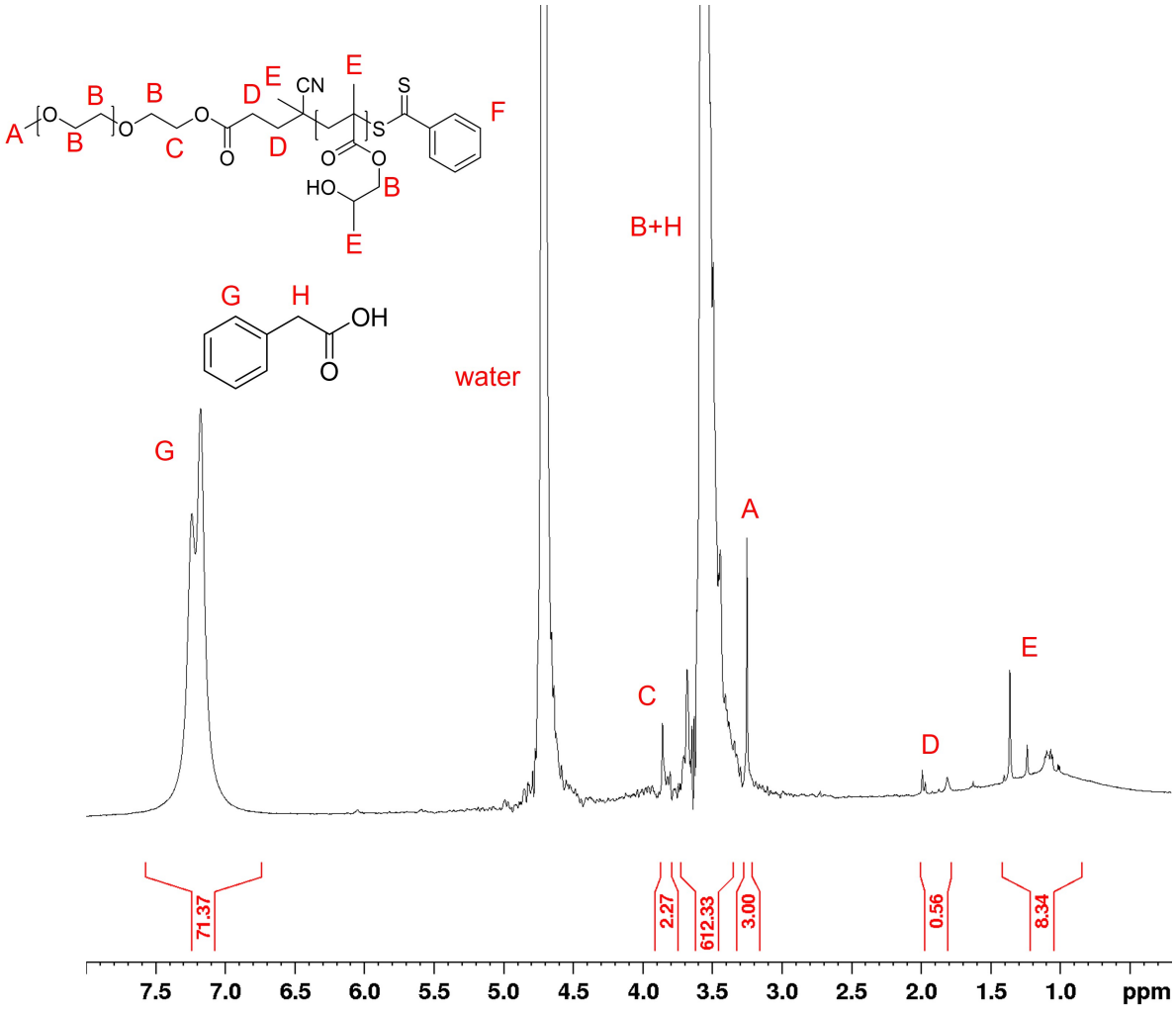

Figure S15. ^{1}H NMR spectrum of PEG-PHPMA 20 in D_2O

S3. ^{1}H NMR diffusion ordered spectroscopy (DOSY) spectra waterfall plots for PEG 10 and PEG-PHPMA 10

Figures S16 and S17 are representative ^{1}H NMR DOSY Waterfall Plots for PEG 10 and PEG-PHPMA 10.

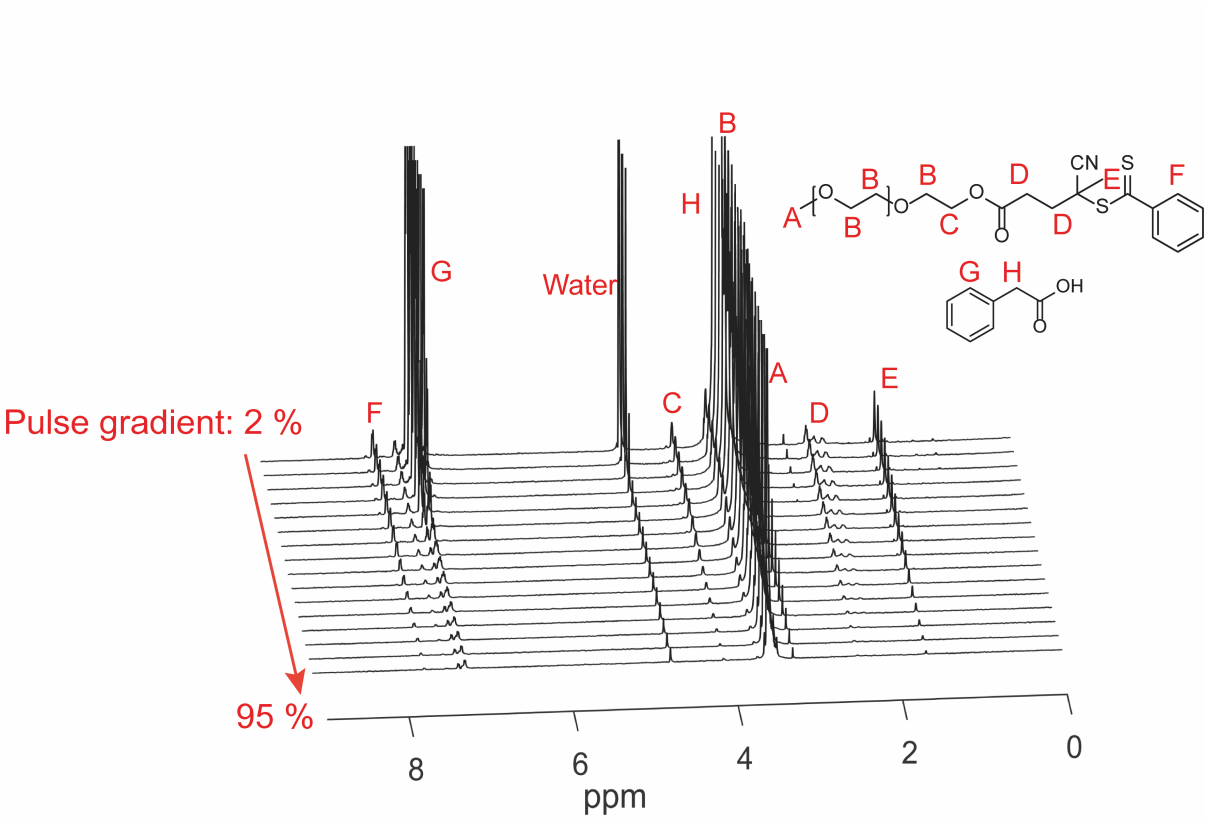

Figure S16. ^{1}H NMR DOSY spectra waterfall plots for PEG 10 in D_2O

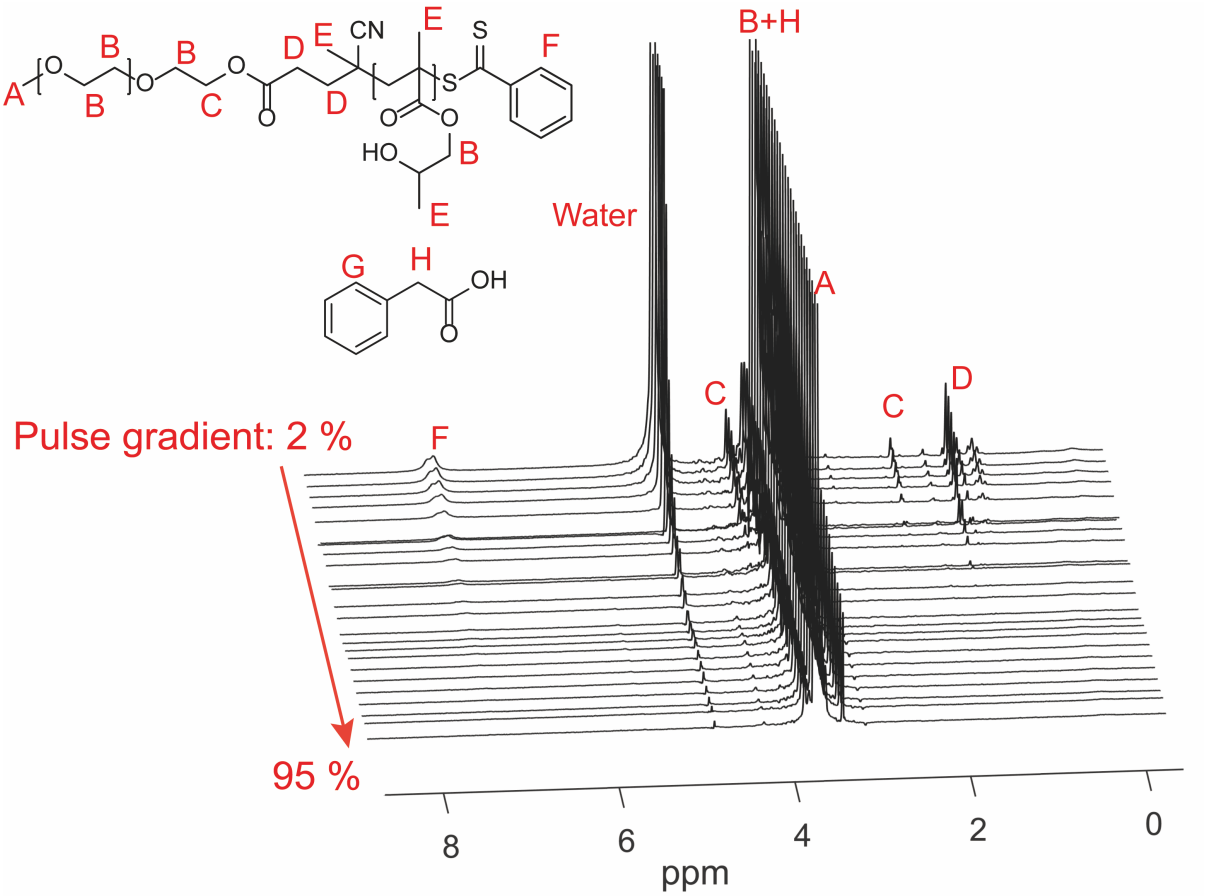

Figure S17. ^{1}H NMR DOSY spectra waterfall plots for PEG-PHPMA 10 in D_2O

S4. ^{1}H NMR DOSY fit parameters for PEG solutions

Figure S18 shows the Eqns. 7 and 9 fits to the PEG 20 ^{1}H NMR DOSY echo decays. Tables S1 to S3 details the ^{1}H NMR DOSY fit parameters for PEG solutions.

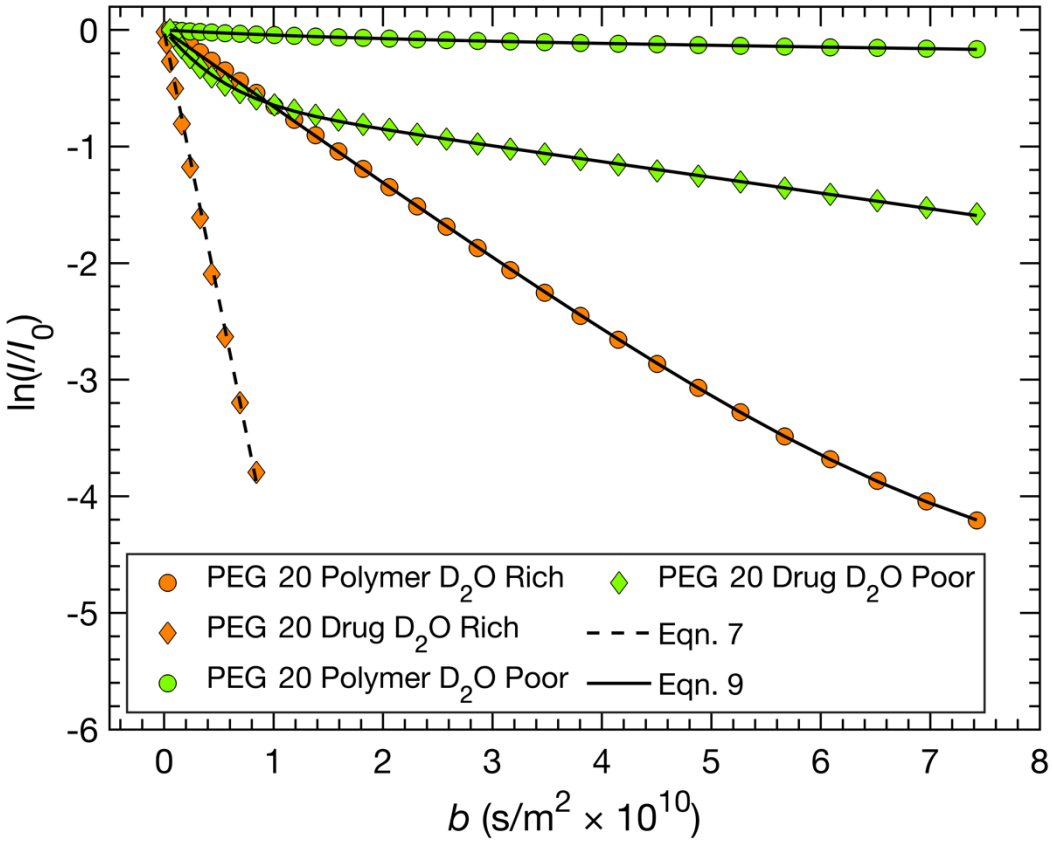

Figure S18. ^{1}H NMR DOSY echo decays for PEG 20

Table S1. ^{1}H NMR DOSY Eqn. 9 fit parameters for PEG Solutions polymer echo decays (Peak B and B')

Sample	f_{DOSY}	$D_{DOSY,1}$ [s/m^2 × 10^{11}]	$D_{DOSY,2}$ [s/m^2 × 10^{11}]
PEG 0	0.99 ± 0.01	6.5 ± 0.1	0.01 ± 0.01
PEG 10	0.84 ± 0.01	6.5 ± 0.1	3.1 ± 0.1
PEG 16 D_2O Rich	0.99 ± 0.01	6.3 ± 0.1	0.2 ± 0.1
PEG 16 D_2O Poor	0.07 ± 0.01	5.4 ± 0.2	0.1 ± 0.1
PEG 20 D_2O Rich	0.99 ± 0.01	6.7 ± 0.1	0.01 ± 0.01
PEG 20 D_2O Poor	0.06 ± 0.01	6.4 ± 0.3	0.1 ± 0.1

Table S2. ^{1}H NMR DOSY Eqn. 7 fit parameters for PA and PEG solutions drug echo decays (Peak G)

Sample	D_{DOSY} [s/m^2 × 10^{11}]
PA 16 mg/mL	67.3 ± 0.2
PEG 10	48.7 ± 0.4

PEG 16 D_2O Rich	45.6 ± 0.6
PEG 20 D_2O Rich	45.8 ± 0.6

Table S3. ^{1}H NMR DOSY Eqn. 9 fit parameters for PEG solutions drug echo decays (Peak G')

Sample	f_{DOSY}	$D_{DOSY,1}$ [s/m^2 × 10^{11}]	$D_{DOSY,2}$ [s/m^2 × 10^{11}]
PEG 16 D_2O Poor	0.43 ± 0.01	23.5 ± 0.9	1.4 ± 0.1
PEG 20 D_2O Poor	0.45 ± 0.01	23.9 ± 0.8	1.4 ± 0.1

S5. ^{1}H NMR DOSY plots and fit parameters for PEG-PHPMA PISA solutions

Figure S19 shows the Eqn. 9 fits to the PEG-PHPMA ^{1}H NMR DOSY Echo Decays. Tables S4 to S6 detail the fit parameters.

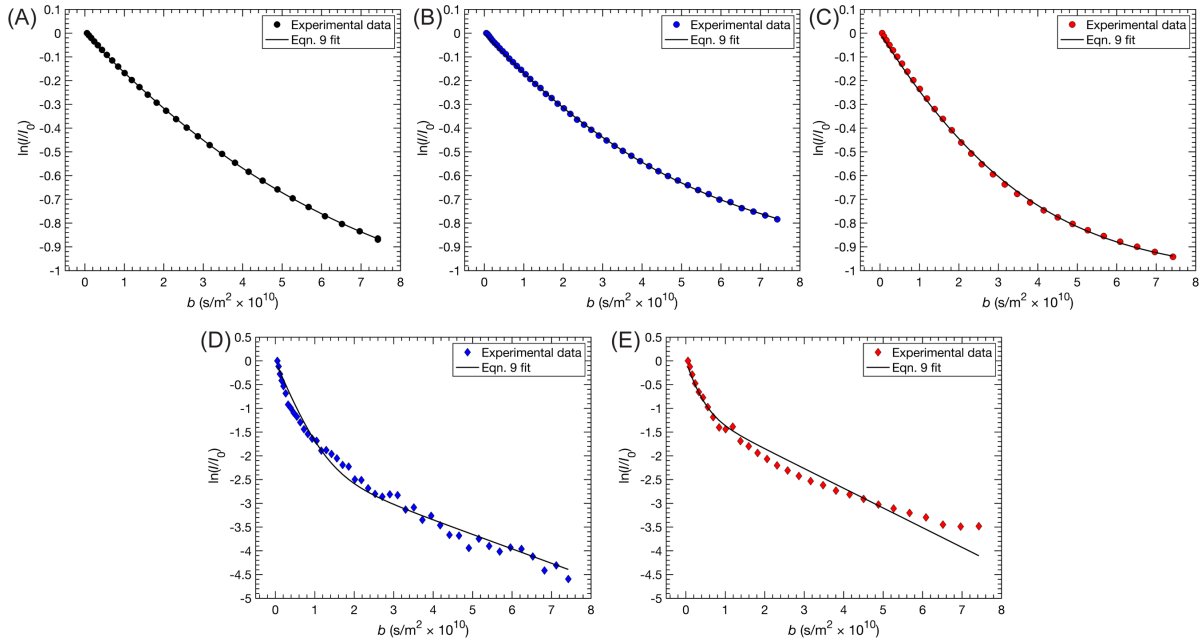

Figure S19. ^{1}H NMR DOSY echo decays for (A) PEG-PHPMA 0 polymer, (B) PEG-PHPMA 10 polymer, (C) PEG-PHPMA 10 drug, and (D) PEG-PHPMA 20 drug. For fitting Eqn. 9 to data depicted in (C) and (D), the drug $D_{DOSY,2}$ = polymer $D_{DOSY,1}$ constraint was employed.

Table S4. ^{1}H NMR DOSY Eqn. 9 fit parameters for PEG-PHPMA PISA solutions polymer echo decays (Peak B)

Sample	f_{DOSY}	$D_{DOSY,1}$ [s/m^2 × 10^{11}]	$D_{DOSY,2}$ [s/m^2 × 10^{11}]
PEG-PHPMA 0	0.63 ± 0.05	2.7 ± 0.2	0.1 ± 0.1

PEG-PHPMA 10	0.58 ± 0.03	3.0 ± 0.1	0.09 ± 0.07
PEG-PHPMA 16	0.62 ± 0.06	3.2 ± 0.3	0.01 ± 0.01
PEG-PHPMA 20	0.64 ± 0.03	3.7 ± 0.2	0.01 ± 0.01

Table S5. ^{1}H NMR DOSY Eqn. 9 fit parameters for PEG-PHPMA PISA solutions drug echo decays (Peak G, drug $D_{DOSY,2}$ is adjustable parameter)

Sample	f_{DOSY}	$D_{DOSY,1}$ [s/m^2 × 10^{11}]	$D_{DOSY,2}$ [s/m^2 × 10^{11}]
PEG-PHPMA 10	0.87 ± 0.01	69 ± 6	4.6 ± 0.2
PEG-PHPMA 16	0.78 ± 0.02	45 ± 5	3.4 ± 0.2
PEG-PHPMA 20	0.82 ± 0.01	28 ± 2	2.9 ± 0.1

Table S6. ^{1}H NMR DOSY Eqn. 9 fit parameters for PEG-PHPMA PISA solutions drug echo decays (Peak G, drug $D_{DOSY,2}$ = polymer $D_{DOSY,1}$ constraint applied)

Sample	f_{DOSY}	$D_{DOSY,1}$ [s/m^2 × 10^{11}]
PEG-PHPMA 10	0.88 ± 0.01	22 ± 1
PEG-PHPMA 16	0.72 ± 0.02	28 ± 3
PEG-PHPMA 20	0.70 ± 0.03	30 ± 4

S6. ^{1}H NMR DOSY fit parameters for water

Table S7 details the Eqn. 7 fit parameters for ^{1}H NMR DOSY echo decays for the water peak.

Table S7. ^{1}H NMR DOSY Eqn. 7 fit parameter for PA, PEG, and PEG-PHPMA solutions water echo decays

Sample	$D_{DOSY,H2O}$ [s/m^2 × 10^{11}]
PA 16 mg/mL	180 ± 10
PEG 0	160 ± 10
PEG 10	160 ± 10
PEG 16	160 ± 10
PEG 20	160 ± 10
PEG-PHPMA 0	130 ± 10
PEG-PHPMA 10	110 ± 10
PEG-PHPMA 16	90 ± 10
PEG-PHPMA 20	110 ± 10

S7. PEG-PHPMA PISA solution viscosity adjustment

To account for the increase in bulk viscosity in the PEG-PHPMA PISA solution, the diffusion coefficients for PA in D_2O without polymer ($D^*_{PA,D2O}$) and PEG aggregates (D^*_{agg}) were adjusted using Eqns. S1 and S2

$$D^*_{PA,D2O} = D_{PA,D2O}\frac{D^*_{DOSY,H2O}}{D_{DOSY,H2O}} \quad \text{(S1)}$$

$$D^*_{agg} = D_{agg}\frac{D^*_{DOSY,H2O}}{D_{DOSY,H2O}} \quad \text{(S2)}$$

where $D_{DOSY,H2O}$ is the average water diffusion coefficient in the PEG solutions and $D^*_{DOSY,H2O}$ is the average water diffusion coefficient in the PEG-PHPMA PISA solutions. $D_{PA,D2O}$ was determined from the 16 mg/mL phenylacetic acid in D_2O solution. D_{agg} corresponds to the PEG $D_{DOSY,2}$ value determined from the PEG solutions.

S8. PEG-PHPMA UV size-exclusion chromatography (SEC) trace deconvolution

UV SEC traces of PEG-PHPMA block copolymer were deconvoluted using custom Matlab scripts. First, Eqn. S3 was fit to the UV SEC trace intensity of the PEG macro-RAFT agent (I_{SEC})

$$I_{SEC} = I_0\left(\frac{f_L/\pi}{1+\left(\frac{t-t_0}{\gamma}\right)^2} + \frac{(1-f_L)}{\sigma\sqrt{2\pi}}\exp\left(-\frac{1}{2}\frac{(t-t_0)}{\sigma^2}\right)\right) + BG \quad \text{(S3)}$$

where t is the retention time, t_0 is the peak time, I_0 is the maximum peak height, f_L is the fractional contribution of the Lorentzian term, γ is the width of the Lorentzian term, σ is the standard deviation of the Gaussian term, and BG is a background term. Then, Eqn. S3 was fit to the UV SEC trace intensity of each PEG-PHPMA block copolymer sample ($I_{PEG-PHPMA}$)

$$I_{PEG-PHPMA} = I_{BCP} + I_{PEG} + BG \quad \text{(S4)}$$

where I_{BCP} and I_{PEG} correspond to the block copolymer and unreacted PEG macro-RAFT agent peaks, respectively. Both I_{BCP} and I_{PEG} are described using the first term in Eqn. S3. To reduce the number of adjustable fit parameters when fitting Eqn. S4 to the PEG-PHPMA data, the f_L, γ, and σ values estimated from the PEG SEC trace are used for the I_{PEG} term.

Figure S20 shows the UV SEC trace deconvolution for PEG-PHPMA 0. Table S8 lists the deconvolution parameters for the PEG-PHPMA PISA samples. $M_{N,BCP}$ and $Đ_{BCP}$ are the number average molar mass and dispersity of the PEG-PHPMA block copolymer peak. $I_{BCP,0}$ and $I_{PEG,0}$ represent the maximum heights of the PEG-PHPMA block copolymer and unreacted PEG macro-RAFT agent peaks, respectively.

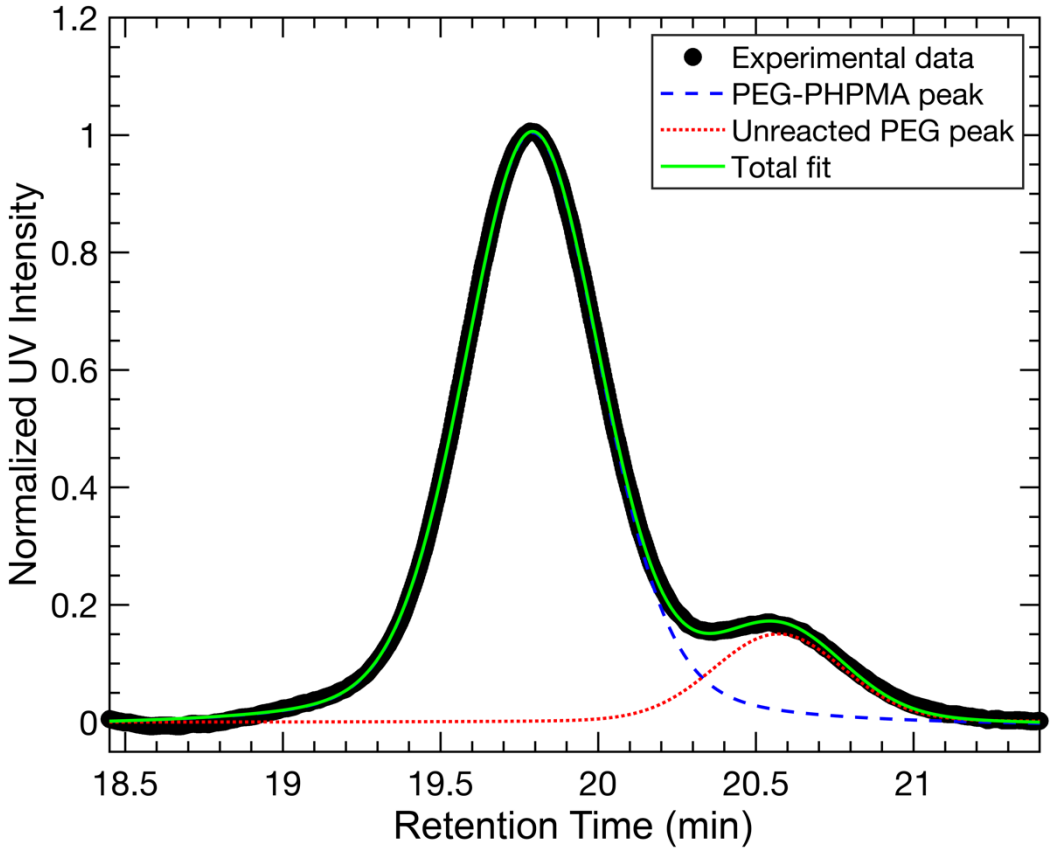

Figure S20. Deconvolution of PEG-PHPMA 0 UV SEC trace

Table S8. PEG-PHPMA molar mass properties

Sample	$M_{N,BCP}$ [kg/mol]	$Đ_{BCP}$	$\frac{I_{PEG,0}}{I_{BCP,0}+I_{PEG,0}}$
PEG-PHPMA 0	12.6	1.09	0.11
PEG-PHPMA 10	12.7	1.13	0.09
PEG-PHPMA 16	13.9	1.14	0.08
PEG-PHPMA 20	12.7	1.12	0.14

S9. PEG-PHPMA PISA kinetics

Figure S21 depicts PISA kinetics data for PEG-PHPMA 0, PEG-PHPMA 10, and PEG-PHPMA 20 samples.

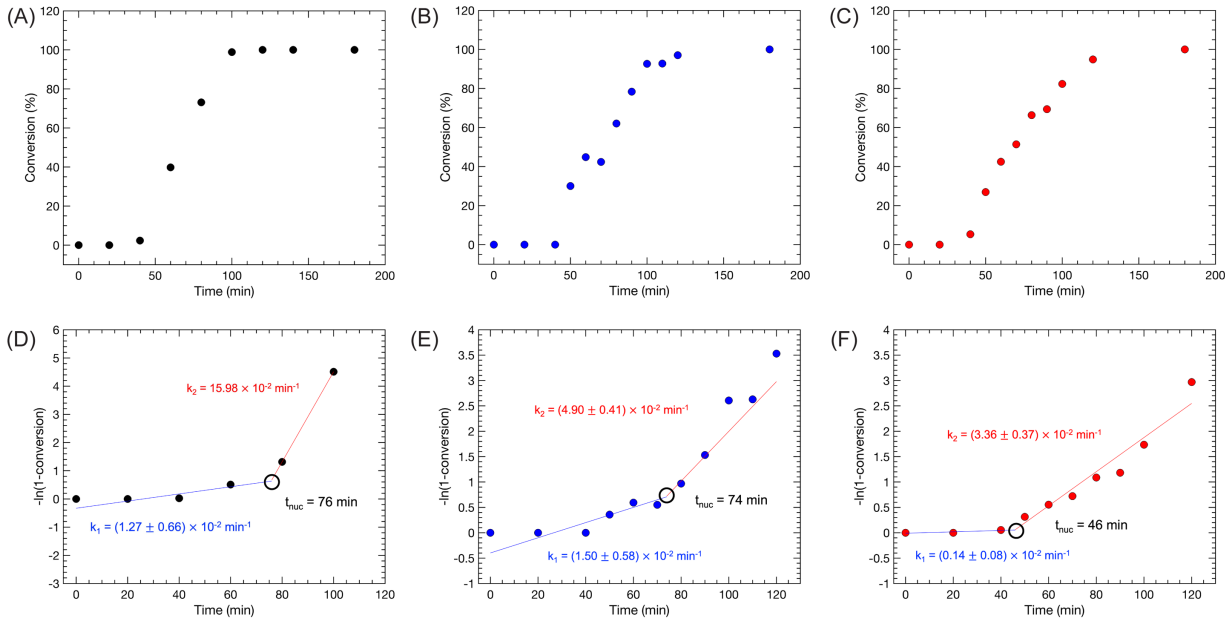

Figure S21. PEG-PHPMA PISA kinetics. HPMA conversion vs. time for (A) PEG-PHPMA 0, (B) PEG-PHPMA 10, and (C) PEG-PHPMA 20. First order kinetics plot for (D) PEG-PHPMA 0, (E) PEG-PHPMA 10 and (F) PEG-PHPMA 20

S11. Impact of initiator concentration on PEG-PHPMA PISA

To investigate the source of the unreacted PEG chains that remain during PISA, preliminary investigations were performed on PEG-PHPMA block copolymers. The targeted PHPMA degree of polymerization was 90.

Figure S22 and Table S9 depict the UV SEC trace of PEG-PHPMA block copolymers prepared by PISA with varying PEG macro-RAFT agent to AIPD initiator ratio ([RAFT]:[AIPD]). For this experiment, [RAFT] was kept constant at 0.036 M and [AIPD] was decreased. In general, the number of terminated chains produced by RAFT polymerization should decrease as [RAFT]:[AIPD] increases.[S1] That trend, however, is not observed in Figure S21. Rather, increasing [RAFT]:[AIPD] from 3:1 to 6:1 does not affect the unreacted PEG shoulder observed near 20.5 min. Increasing the ratio to 10:1 leads to a very large shoulder, as the rate of HPMA polymerization is greatly reduced. Decreasing the [RAFT]:[AIPD] to 1.5:1 leads to a slightly larger PEG-PHPMA molar mass, but a large fraction of unreacted PEG RAFT agent remains. Along with the presence of the UV-active CPPA end group on the chains, the insensitivity towards the [RAFT]:[AIPD] ratio demonstrates that the unreacted PEG chains have not undergone termination.

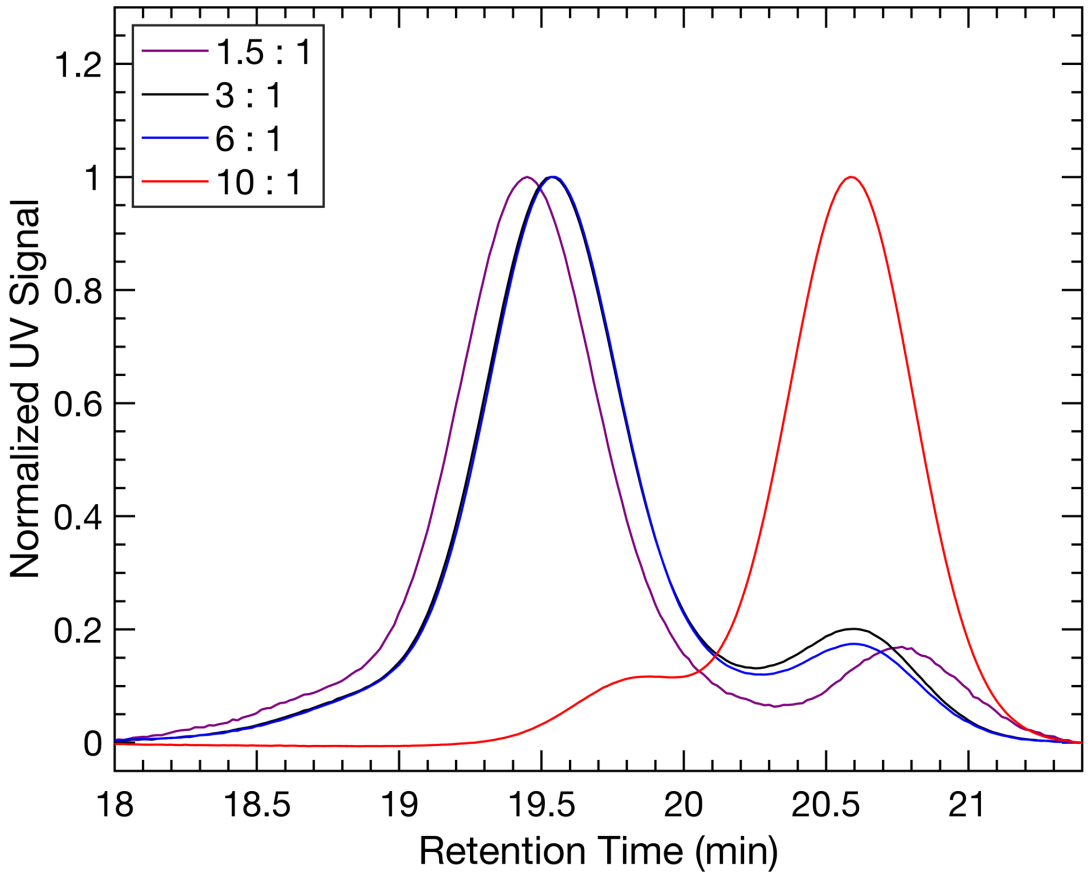

Figure S22. UV SEC trace of PEG-PHPMA produced by PISA with varying [RAFT]:[AIPD] ratios. The targeted PHPMA degree of polymerization was 90

Table S9. Molar mass characterization of PEG-PHPMA produced by PISA with varying [RAFT]:[AIPD] ratios. The targeted PHPMA degree of polymerization was 90

[RAFT]:[AIPD] ratio	$\boldsymbol{M_{N,BCP}}$ **[kg/mol]**	$Đ_{BCP}$	$\frac{I_{PEG,0}}{I_{BCP,0}+I_{PEG,0}}$
1.5:1	18.3	1.14	0.11
3:1	15.3	1.16	0.12
6:1	15.2	1.16	0.10
10:1	8.83	1.44	0.88

S12. Impact of free PEG-OH chains on PEG-PHPMA PISA

To explore the impact of free PEG chains within the PISA solution, PEG-PHPMA 0 PISA reactions were performed in the presence of PEG-OH chains, which do not participate in PHPMA polymerization because they lack the CPPA end group.

Figure S23A shows the UV SEC of PEG-PHPMA 0 samples containing 0.5 and 1 eq. of PEG-OH relative to the PEG macro-RAFT agent. UV SEC, which does not detect PEG-OH, indicates that the PEG-PHPMA 0 molar mass distribution is unperturbed by the additional free chains. Figure S23B demonstrates that the free PEG-OH does not significantly affect the R_h distribution of the micelles, as observed by DLS. Figure S23C depicts ^{1}H NMR DOSY decays of the PEG-PHPMA and PEG-OH solutions. Due to the biexponential shape, Eqn. 9 was fit to each echo decay (see Table S9 for fit parameters). For the fast diffusion mode, the samples containing additional PEG-OH each produce $D_{DOSY,1} \approx 2.5 \times 10^{-10}$ m^2/s. f_{DOSY}, however, increases with increasing PEG-OH amounts. This relationship suggests that the fast diffusion mode observed by ^{1}H NMR DOSY describes the diffusion of both PEG-PHPMA micelles and PEG unimer chains. The slow diffusion mode produces $D_{DOSY,2} \lessapprox 1 \times 10^{-13}$ m^2/s.

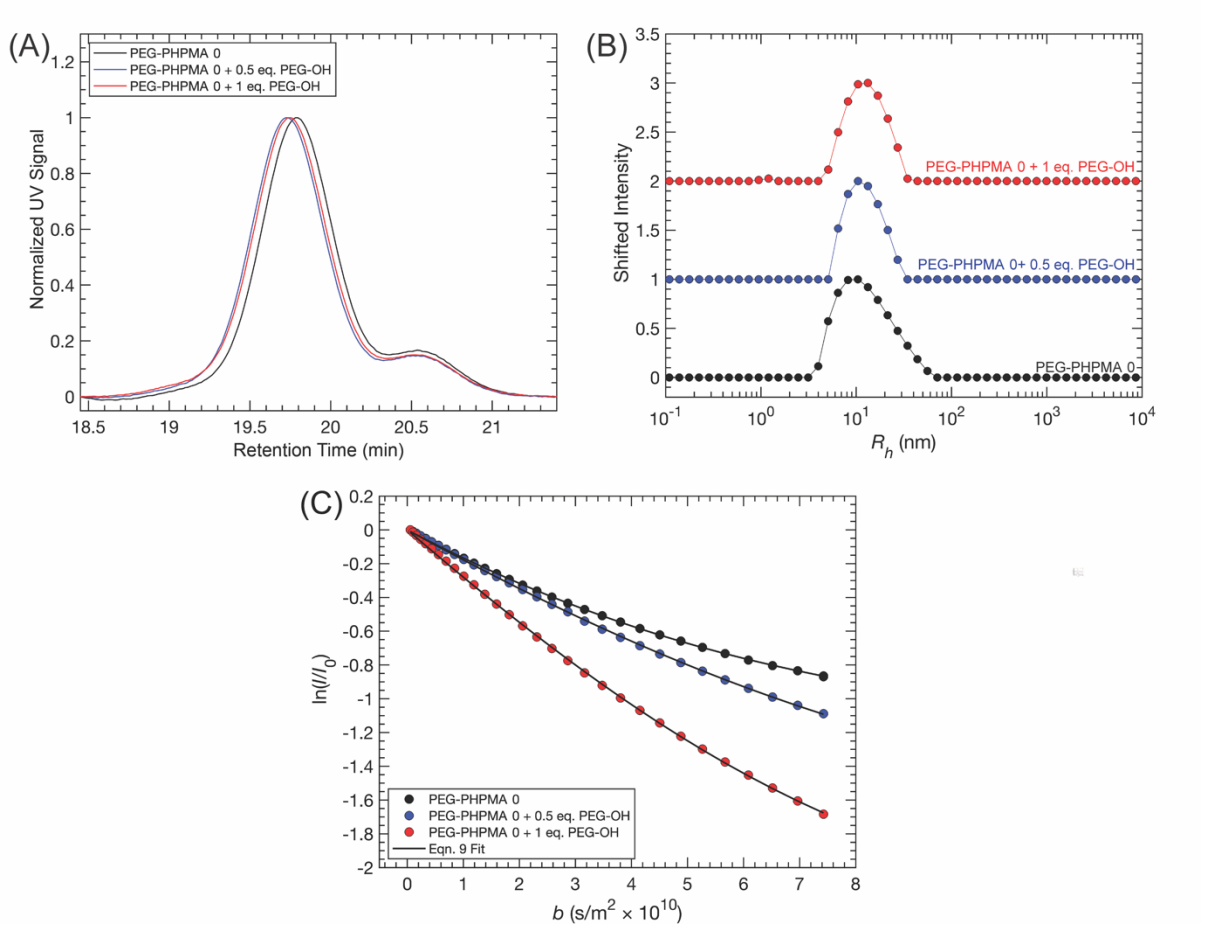

Figure S23. Characterization of PEG-PHPMA 0 PISA solutions with varying amounts of additional PEG-OH. (A) UV SEC, (B) DLS R_h distributions, and (C) ^{1}H NMR DOSY polymer echo decays

Table S9. ^{1}H NMR DOSY Eqn. 9 Fit Parameters for PEG-PHPMA PISA Solutions Polymer Echo Decays (Peak B)

Sample	f_{DOSY}	$D_{DOSY,1}$ [s/m^2 × 10^{11}]	$D_{DOSY,2}$ [s/m^2 × 10^{11}]
PEG-PHPMA 0 + 0.5 eq. PEG-OH	0.82 ± 0.05	2.3 ± 0.1	0.01 ± 0.01
PEG-PHPMA 0 + 1.0 eq. PEG-OH	0.88 ± 0.04	3.2 ± 0.3	0.2 ± 0.4

S13. PEG 0 DLS hydrodynamic radius distribution

Figure S23 is the PEG 0 DLS R_h distribution with the intensity axis enlarged.

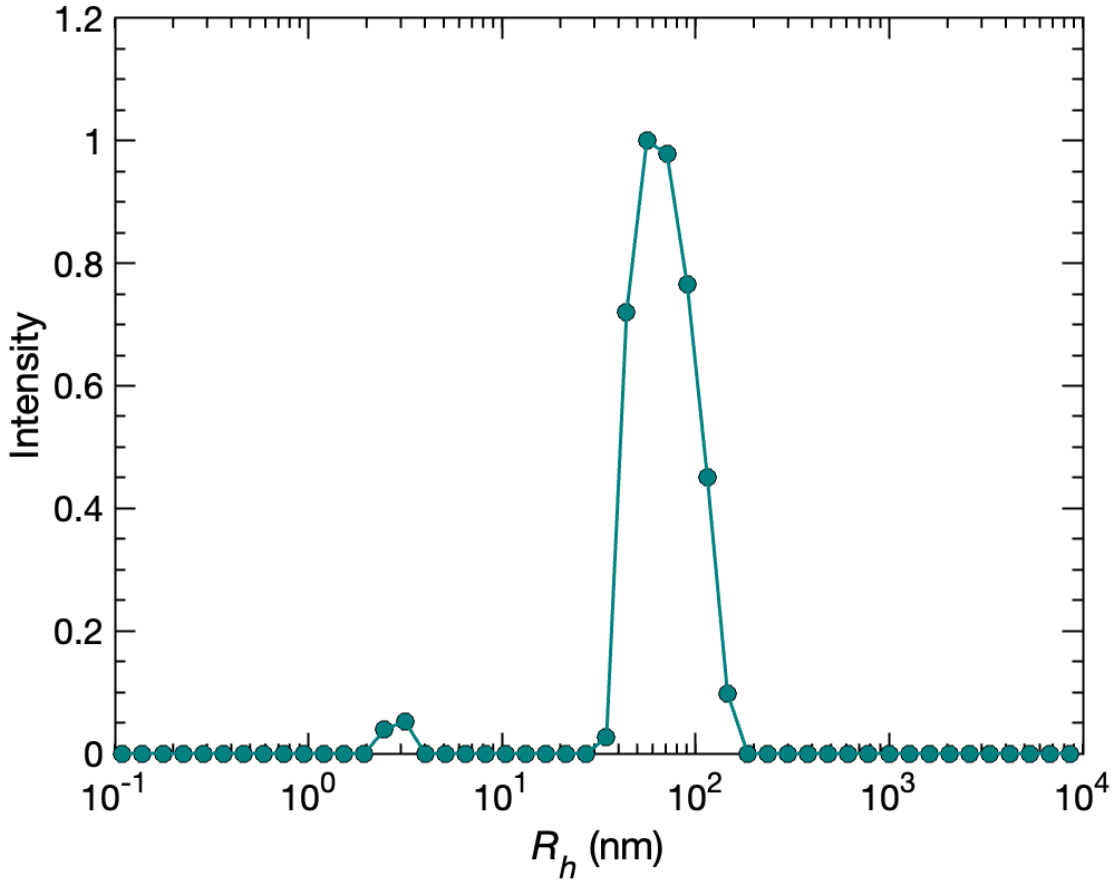

Figure S24. PEG 0 DLS R_h distribution

S14. Eqn. 10 derivation

The fraction of PA bound to the PGMA-PHPMA nanoparticles was estimated using the two-state model

$$D_{DOSY} = p_{agg}D_{agg} + (1 - p_{agg})D_{PA,DOSY} \quad \text{(S5)}$$

In this model, the observed PA diffusion coefficient D_{DOSY} is assumed to be a weighted average of the fraction of drug bound to a PEG aggregate and the fraction that is freely dissolved. D_{agg} is the diffusion coefficient of the polymer-drug aggregate, p_{agg} is the mole fraction of drug bound to the aggregate, and $D_{PA,DOSY}$ is the diffusion coefficient of freely dissolved drug.[S2] Eqn. S5 may be rearranged to solve explictly for p_{agg}, as depicted in Eqn. 10 in the main manuscript.

S15. Estimated hydrodynamic radii and diffusing species

Tables S10 – S12 depict the ^{1}H NMR DOSY estimated R_h and diffusing species for the PEG and PEG-PHPMA solutions. For the PA signal (Peak G) detected in the PEG 10, PEG 16 D_2O Rich, PEG 20 D_2O Rich, and PEG-PHPMA samples, an R_h table is not provided because the observed diffusion coefficient reflects both the drug freely dissolved and the drug bound to aggregates.

Table S10. ^{1}H NMR DOSY estimated R_h and diffusing species for PEG Solutions polymer echo decays (Peak B and B')

Sample	$R_{h,1}$ [nm]	$R_{h,1}$ Diffusing Species	$R_{h,2}$ [nm]	$R_{h,2}$ Diffusing Species
PEG 0	3.0 ± 0.1	Unimers	> 2000	Aggregates
PEG 10	3.0 ± 0.1	Unimers	7.0 ± 0.2	Aggregates
PEG 16 D_2O Rich	3.1 ± 0.1	Unimers	100 ± 100	Aggregates
PEG 16 D_2O Poor	3.5 ± 0.1	Unimers	151 ± 4	Aggregates
PEG 20 D_2O Rich	2.9 ± 0.1	Unimers	> 2000	Aggregates
PEG 20 D_2O Poor	3.1 ± 0.1	Unimers	158 ± 5	Aggregates

Table S11. ^{1}H NMR DOSY estimated R_h and diffusing species for PEG solutions drug echo decays (Peak G')

Sample	$R_{h,1}$ [nm]	$R_{h,1}$ Diffusing Species	$R_{h,2}$ [nm]	$R_{h,2}$ Diffusing Species
PEG 16 D_2O Poor	0.9 ± 0.1	Drug interior to aggregates	16 ± 1	Drug exterior to aggregates
PEG 20 D_2O Poor	0.9 ± 0.1	Drug interior to aggregates	16 ± 1	Drug exterior to aggregate

Table S12. ^{1}H NMR DOSY estimated R_h and diffusing species for PEG-PHPMA PISA solutions polymer echo decays (Peak B)

Sample	$R_{h,1}$ [nm]	$R_{h,1}$ Diffusing Species	$R_{h,2}$ [nm]	$R_{h,2}$ Diffusing Species
PEG-PHPMA 0	7.3 ± 0.4	Micelles and unimers, and aggregates	200 ± 100	Aggregates
PEG-PHPMA 10	6.4 ± 0.3	Micelles, unimers, and aggregates	200 ± 200	Aggregates
PEG-PHPMA 16	6.1 ± 0.5	Micelles, unimers, and aggregates	> 2000	Aggregates
PEG-PHPMA 20	5.3 ± 0.9	Micelles, unimers, and aggregates	> 2000	Aggregates

S16. Transmission electron microscopy particle size distributions

Figure S25 depicts the particle size distributions obtained from transmission electron microscopy.

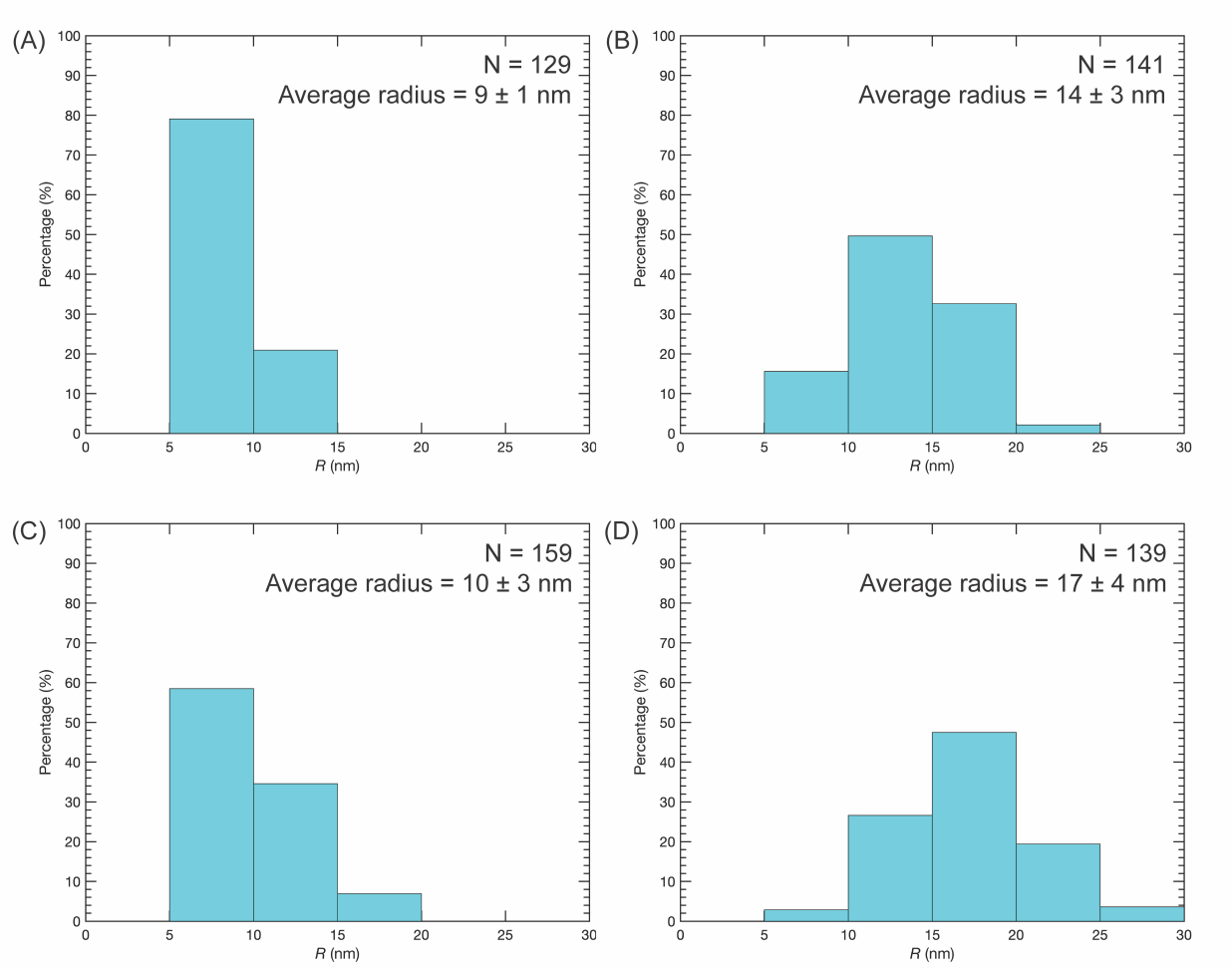

Figure S25. Transmission electron microscopy particle size distributions for (A) PEG-PHPMA 0, (B) PEG-PHPMA 10, (C) PEG-PHPMA 16, and (D) PEG-PHPMA 20. *N* refers to the total number of particles represented in the distribution

S17. References

[S1]S. Perrier, *Macromolecules*, 2017, **50**, 7433–7447.

[S2]G. Li, D. C. Barzycki, and R. G. Ricarte, *AIChE J.*, 2023, **69**, e18014.